Optimization of the Automatic Steering Control of a Vehicle in a Guideway With Positive Mechanical Retention

T. L. Lague, Rohr Industries, Inc.

This paper addresses automatic steering with the objective of taking maximum advantage of a positive constraint guideway. Two steering approaches are examined for stability: ride quality (sensitivity of acceleration at the passenger location to guidance source irregularities) and average error as it impacts on guideway width. The influence of system gain and compensation, dynamic characteristics of a wall-following suspension, and dynamics of the steering mechanism itself are examined. They are found to have an important influence on both stability and ride quality. Most of the analysis uses conventional small perturbation linear models. Transfer functions in the Laplace operator are generated to evaluate stability and the spectral densities of acceleration at the passenger location. Error is evaluated from these representations plus equilibrium determinations by using the nonlinear force relations.

The main thrust of our lateral guidance design effort has been to take maximum advantage of the requirement for positive mechanical retention in switches. Can the positive retention requirement be exploited to simplify or improve performance and reliability of the automatic steering system? This study takes the first cut at this question by exploring some of the basic dynamic relations. The work known or available to us that bears on this problem has been limited to servocontrolled vehicles on open roadway, notably the work at Ohio State University. Our study, which to date has remained analytical, has sought to develop a computer model of the free-running vehicle, which includes the coupled dynamics of the steering mechanism.

The two approaches compared in the study might be considered extremes of active and passive lateral control. The results show enough attractive possibilities in the more passive approach to encourage continued analysis and verification tests.

OBJECTIVES

Two basic approaches to steering are compared. The primary measure of comparison is ride quality. The comparison is made within specific boundaries on turn performance and control system stability. Outside the scope of this report, the approaches have been compared in terms of system complexity, safety, reliability, maintainability, and initial cost.

The objective of this study is to define and compute specific quantitative measures of performance and constraints that can ultimately be measured in the operational vehicle. The ride quality measure is the total root mean square (rms) value of acceleration at a passenger location in response to a given amplitude and frequency spectrum of random guideway irregularity. The turn performance measure is dual. The primary measure is steady-state error in a turn; the secondary measure is low-frequency response in following a reversing turn path. The stability measure requires maintaining a specific damping ratio in all oscillatory modes.

APPROACH

This study compares the practical range of the important design parameters of two steering systems. Small perturbation dynamic analysis is used to model the system shown in Figure 1. In a quantitative comparison, the following specific measures must be established for each of the qualities and constraints outlined in the study objectives:

1. Ride quality measure (acceleration at the passenger location);
2. Guideway model;
3. Stability measure;
4. Turn performance measure (steering accuracy); and
5. Mathematical model of the vehicle, steering dynamics, and control system.

The ride quality model is the performance measure. The stability and turn performance measures are intended to provide for ride quality comparison on an equal footing. They constitute go-no go tests.

Ride Quality Measure

Ride quality is the key standard for comparison. It measures the output of the system that results from the guideway model input. The guideway model that is defined here is really a model of the unwanted irregularities in the guideway that are processed by the vehicle to generate unwanted time variation of acceleration at the passenger location. This time variation of acceleration is superimposed on lateral acceleration patterns

that are required of the vehicle in following the required path. Control of these required accelerations, usually referred to as sustained acceleration, is properly a concern of guideway design and is not addressed in this study.

The objective here is to establish the form of the unwanted acceleration measure and the acceptable amplitude. For our purpose, which is a parametric evaluation, to reduce the measure to a single number that is compatible with a realistic guideway representation would be advantageous. Considerable test data have accumulated on human tolerance to periodic (sinusoidal) motion—acceleration as a function of frequency. Hanes (1) gives an excellent review of the data accumulated to 1970. The International Organization for Standardization (ISO) has set limits for human exposure to acceleration based on the accumulated data. The latest recommendations for lateral acceleration (2) are shown in Figure 2. The recommendations are based on evaluations of fatigue decreased proficiency that has been reduced by approximately a factor of 3 to arrive at the reduced comfort boundary. The extension of lateral recommendations to lower frequencies is new and is not duplicated in the ISO recommendations for vertical acceleration. For comparison, the 20-min exposure curve for vertical is shown in Figure 2 as a dashed line.

In tests for this relation, the human response data are in the form of acceleration amplitude as a function of frequency because the straightforward thing to do is to shake people at a discreet frequency and amplitude and to repeat the process until the desired frequency and amplitude range is covered. This is obviously a proper test procedure because it yields exactly the desired relation among the variables.

Those charged with specifying ride quality naturally prefer to use the best available human tolerance data directly; therefore, they usually specify ride quality in terms of allowable acceleration (either peak or rms) as a function of frequency. This presents a considerable difficulty when the specification must be used in design or when real-world vehicles must be tested for specification compliance.

In the first case, design, to introduce a sinusoidal input into the system model and generate a sinusoidal acceleration is a simple matter. This, however, serves only to pass the problem on to selection of a guideway model in which the sinusoidal representation is quite unrealistic. It can be said without reservation that a periodic guideway is a poor guideway. Matters are further complicated by providing a ride quality measure that is a multivalued function of frequency.

In the second case, specification compliance, the test data are approached with the question, At what frequency is this body shaker operating? Good vehicles (poor shakers) get difficult to evaluate. The formulation has worked fairly well for some rail systems.

Acceleration data are reduced in a quasi-objective manner to produce acceleration levels at discreet frequencies depending on the operating condition and roadbed. If the vehicle suspension system is poorly damped or its structure possesses a high capability for amplifying specific frequency content of the input or both, the vehicle provides the periodicity.

Only in the special case of elevated spans does a well-designed guideway present a periodic input to a passing vehicle. In that case it results from the pier encounter and the bending frequencies of the beams. Lateral guidance excludes even these special cases. Thus, the unwanted guidance irregularities that may be transmitted by the lateral guidance system are nonperiodic. If the guidance system is adequately damped and the vehicle structure is well designed, we can anticipate essentially nonperiodic motions at the passenger location.

As a consequence of the foregoing, we have devised this procedure for arriving at a relative performance ride quality measure expressed as a single value and capable of being measured in a performance test under operating conditions.

1. The guideway input is proportional and defined as a spectrum A/Ω^2.
2. The ride quality measure is the weighted rms value of the random acceleration at a selected passenger location, the total over the frequency range of concern. The weighting is the inverse of the ISO comfort boundary extended at low frequency as shown in Figure 2. The rms value is obtained in the parametric analysis by integrating the spectrum over the frequency range. In actual vehicle tests the rms value would be obtained by integrating the time history of the acceleration. The two are equivalent if the real-world acceleration is filtered to confine its content to the spectrum frequency range, C.

$$(\ddot{y}_p)^2 = \int_C \Phi(\omega)\, d\omega = \frac{1}{T}\int_0^T \ddot{y}\,(t)^2\, dt \qquad (1)$$

This formulation of the measure provides one number to indicate the systems performance over the frequency range. It is an absolute as well as a relative measure since it can be compared directly with the ISO recommendation. That is, this measure will reduce to a comparison with the specification if the output is concentrated at a discreet frequency within the spectrum frequency range and the comparison is made at the amplitude where the weighting factor is normalized. We used the weighting factor, W, defined as follows:

$$W = \left(\frac{\omega}{2\pi}\right)^{1/2} \quad \text{for } \omega < 2\pi$$

$$W = 1 \quad \text{for } 2\pi < \omega < 4\pi$$

$$W = \frac{2\pi}{\omega} \quad \text{for } \omega > 4\pi \qquad (2)$$

Thus the comparison value is the constant acceleration region between 1 and 2 Hz. This extrapolation of the ISO recommendation down to 0.1 Hz is conservative in our judgment.

Guideway Model

The model described here was formulated in another report (3). Data accumulated on prepared road and runway surfaces lead to the conclusion that the random difference in height between two points is proportional to the horizontal distance between them. This may not hold over an extreme horizontal range, but it is a good approximation to prepared surfaces within the range of horizontal distances where height differences might be classified as unwanted irregularities and where they are important to ride quality at ground transportation speeds.

If irregularities are assumed to be random, this proportional characteristic can be represented by a spatial spectral density proportional to the square of the wavelength. Thus, if a spatial frequency is defined as

$$\Omega = \frac{2\pi}{\lambda} \qquad (3)$$

where λ = wavelength, the squared amplitude spectral density can be defined as

$$\Phi_g(\Omega) = \frac{A}{\Omega^2} \quad (4)$$

where A is the roughness measure and the variable change provides a convenient frequency representation. The redeeming quality of Ω is its simple relation to time frequency. $\omega = U\Omega$ when height variation as a function of time is generated by passing over the surface at velocity, U. We have selected for use as input $A = 1.5 \times 10^{-5}$ ft·rad. This is three times as rough as an excellent airport runway. The value of A as it relates to existing surfaces has been fairly well established by actual measurement. There is some confusion as to how a specific value may be translated into a practical guideway construction standard.

The guideway spectrum is converted into a density with respect to time frequency ω:

$$\Phi_g(\omega) = \frac{A}{\omega^2} U \quad (5)$$

This is the input to the vehicle model for the study comparisons of acceleration at the passenger location.

Stability Measure

For our purposes, damping must always meet a more stringent requirement than stability. It is not within the scope of this paper to examine stability margins in terms of system deterioration or malfunction; however, for the servo system, gain margins of 2.0 and 0.5 can be nominally met for all the accepted configurations. The fundamental damping standard has been set at $\zeta > 0.25$. Higher damping will be used unless a significant ride quality trade-off is evident.

Turn Performance Measure

Perfect turn performance is accomplished when the vehicle follows the intended path exactly. Reasons for departing the guideway center are built into front-wheel steering and will be common to all such systems. Drift to establish turning (centrifugal) force from the tires and Ackerman tracking are the most important. This study is concerned only with those error sources that result from the performance of the automatic steering system. We use two measures of this performance:

1. The steady-state system error and
2. The low-frequency response error.

The first cannot be obtained accurately from the small perturbation equations; however, for the two systems studied, simple approximations are available. These are described later. The second can be derived from the low-frequency lag of the system. Repeated reversing curves in a guideway can be approximated by a sinusoidal path lying in a horizontal plane. Bounds can be placed on the sinusoidal as follows: Any curve entry (transition) would be constrained by the jerk specification. The curve radius would be constrained by the lateral acceleration specification. For our purposes, a flat turn has been assumed. Within these limitations, the lateral departure from guideway centerline can be computed as follows from the geometry as shown in Figure 3.

$$\omega = 2\pi f = 2\pi U/L \quad (6)$$

If the lateral component of the centerline is $y = Y \sin(\omega t)$ and the lagged path is $y' = Y \sin(\omega t + \phi)$, it can be shown that Δy is max at $\omega t = -\phi/2$. The total lateral departure is $\Delta y = 2Y \sin \phi/2$.

$$\ddot{y} = \omega^2 y, \dddot{y} = \omega^3 y \quad (7)$$

where

$\ddot{y}$ = max lateral acceleration and
$\dddot{y}$ = max jerk.

By this measure, $Y = \ddot{y}/\omega^2$ when $\omega < \ddot{y}/\dddot{y}$, $Y = \dddot{y}/\omega^3$ when $\omega > \ddot{y}/\dddot{y}$, and $\ddot{y} = \dddot{y} = 3.22\ (0.1\ g)$. The test path for low-frequency response will be defined by the acceleration limit when $\omega < \ddot{y}/\dddot{y}$ and by the jerk limit when $\omega > \ddot{y}/\dddot{y}$. Conveniently both limits are 0.1, giving a crossover frequency of 1 rad/sec.

For the systems under consideration, it turns out that the error grows linearly with reduced frequency under the constant peak acceleration constraint. We have selected a frequency $\omega = 0.25$ rad/sec as the test point for this measure. At 60 mph, this generates a lateral departure Y of ±52 ft combined with a wavelength, L, of 2,200 ft. When equations 6 and 7 are used, this test point changes with speed.

With the two measures defined thus, an acceptable system must not exceed a steady-state error of 6 in. and a low-frequency lag, Δy, of 5 in.

System Model

The two approaches to steering may be thought of as opposite poles of a range of concepts. The most active extreme is servo steering; the most passive is herd steering. Diagrams of the two systems are shown in Figures 4 and 5.

Servo steering is a straightforward approach in which the wall follower senses the departure of a control point on the vehicle from the desired path by measuring the distance to the wall. This error signal drives the steering angle through a hydraulic-actuated steering angle position servo. Thus the turning force is generated by steering the front wheels. In the pure servo system, the wall follower need not bear a significant force. In fact, it can be replaced by any sensor that can generate a signal proportional to the departure from guideway centerline.

Herd steering requires that the wall follower generate a significant part of the steering force. The primary control loop is passive. The force at the control point generated by the wall follower is reacted to by the front tires. Front steering is lightly castered. Thus, the steering angle changes to follow the new path. The vehicle is "herded" down the guideway with no primary steering angle control. The major advantages of this approach are simplicity, inherent stability, and built-in positive retention.

Persistent high loading of the wall follower can be avoided in turns where significant lateral acceleration must be sustained by adding a trimming loop to the basic system. This is approximately equivalent to proportional plus integral control. A relatively stiff and well-damped centering spring is added to the steering mechanism. The null point of this centering spring is adjusted slowly by a screw jack whenever a consistent error exists. This continually acts to relieve the load on the wall follower.

As previously stated, the two systems represent extremes of a range of concepts. The servo vehicles can

take on characteristics of the herd vehicle as wall-follower stiffness is increased. Linkages from the wall follower can provide primary steering forces or moments. This study treats only parameter variation in herd steering and in servo steering including significant changes in the wall-follower force component.

System Definition

The definitions of symbols and stability derivatives used in the remainder of this paper are given in Tables 1 and 2. Figures 6 and 7 show the systems with the variables defined in both active and passive control loops. The steering servo is represented by an equivalent first-order time lag. Lead compensation is represented by a single zero (rate feedback). In actual practice, the servo actuator transfer function would be more complicated. No doubt the most effective compensation would also be more elaborate. These approximations are considered conservative assumptions to use in assessing the achievable response.

Vehicle Dynamics

The vehicle is represented by three degrees of freedom. Two are body motion: lateral displacement and yaw (rotation about a vertical axis). The third is rotation of the front wheels and steering mechanism. The combined mass and rotational inertia of the steering linkage and wheels are lumped. The coordinates and variables are defined in Figure 8 and in Tables 1 and 2. The basic degrees of freedom are

1. Vehicle lateral motion or sway, y;
2. Vehicle rotation about the vertical axis at the combined center of gravity, or yaw, ϕ; and
3. Front wheel rotation about the kingpin or steering angle, δ.

The conventional "bicycle" representation is used for the vehicle. The slope of the tire characteristic curve at zero steer angle was used to establish force and moment derivatives. The following assumptions apply:

1. Roll steering is negligible,
2. Forward velocity is constant,
3. Yaw moment due to differential vertical tire loading is negligible, and
4. Steering mass is lumped with center of gravity forward of the kingpin as computed from the existing design configuration.

The coupled equations of vehicle rotation and translation-steering rotating and translating mass were written in body coordinates and small perturbed to obtain the following equations:

$$\sum Y = (m)\,\dot{v} + m_s \ell_s\,\ddot{\delta} + U(m)r + m_s(\ell_s + x_1 - x_{cg})\,\dot{r} \tag{8}$$

for lateral force;

$$\sum M = m_s \ell_s\,\dot{v} + I_s\ddot{\delta} + m_s \ell_s U r + [I_s + m_s \ell_s (x_1 - x_{cg})]\,\dot{r} \tag{9}$$

for steering moment; and

$$\sum N = m_s(\ell_s + x_1 - x_{cg})\,\dot{v} + [I_s + m_s \ell_s (x_1 - x_{cg})]\,\ddot{\delta} + m_s(\ell_s + x_1 - x_{cg})\,U r + I\,\dot{r} \tag{10}$$

for vehicle moments about z-axis. When the steering is constrained by an irreversible (load insensitive) servo, these equations reduce to

$$\sum Y = m(\dot{v} + U\,\dot{r}) \tag{11}$$

for lateral force and

$$\sum N = I\,\dot{r} \tag{12}$$

for vehicle moment about z-axis. The force summations are as follows (coefficient definitions are given in Table 1):

$$\sum Y = Y_v v + Y_\delta \delta + Y_{\dot\delta}\,\dot\delta + Y_r r + F_c \tag{13}$$

$$\sum M = M_v v + M_\delta \delta + (K_s + K_{kp})\,\delta + (B_s + M_{\dot\delta})\,\dot\delta + M_r r \tag{14}$$

$$\sum N = N_v v + N_\delta \delta + N_{\dot\delta}\,\dot\delta + N_r r + F_c\,(x_{cc} - x_{cg}) \tag{15}$$

for herd steer. The M sum is eliminated for servo steer.

Transfer Functions

Additional equations are required to define lateral position of the steering point, wall-follower force, control equations, and acceleration at the passenger location.

$$\ddot{y}c = \dot{v} + U\,r + (x_{cc} - x_{cg})\,\dot{r} \tag{16}$$

$$F_c = K_c\,(y_0 - y_c) + B_c\,(\dot{y}_0 - \dot{y}_c) \tag{17}$$

$$\delta_0 = K_I\,(y_0 - y_c) \tag{18}$$

$$\ddot{y}_p = [\dot{v} + U\,r + (x_p - x_{cg})\,\dot{r}]/g \tag{19}$$

$$\delta + \Upsilon_c\dot{\delta} = G_c\,(y_0 - y_c) + G_c\Upsilon_0\,(\dot{y}_0 - \dot{y}_c) \tag{20}$$

These equations were written in the Laplace operator, assembled in a small digital computer program to form matrix equations.

$$[C] \times \begin{bmatrix} v \\ \delta \\ r \\ y_c \\ F_c \\ \delta_0 \end{bmatrix} = y_0\,[I] \times \begin{bmatrix} 0 \\ 0 \\ 0 \\ 0 \\ K_c + B_c s \\ K_I s \end{bmatrix} \tag{21}$$

for the herd steering system and

$$[C] \times \begin{bmatrix} v \\ \delta \\ r \\ y_c \\ F_c \\ \delta_0 \end{bmatrix} = y_0\,[I] \times \begin{bmatrix} 0 \\ G_c(1 + \Upsilon_0 s) \\ 0 \\ 0 \\ K_c + B_c s \\ 0 \end{bmatrix} \tag{22}$$

for the servo steering system, where the typical element of C is a polynomial in s. The determinant of C, a polynomial in s, is the characteristic equation of the closed-loop transfer function. Root loci are obtained from the characteristic equation. The transfer function $\ddot{y}_p/y_0(s)$ is used to obtain the acceleration at the passenger location by operating on the guideway model. $j\omega$ is substituted for s to obtain the equivalent of the Fourier transform as follows:

Figure 1. Guidance system.

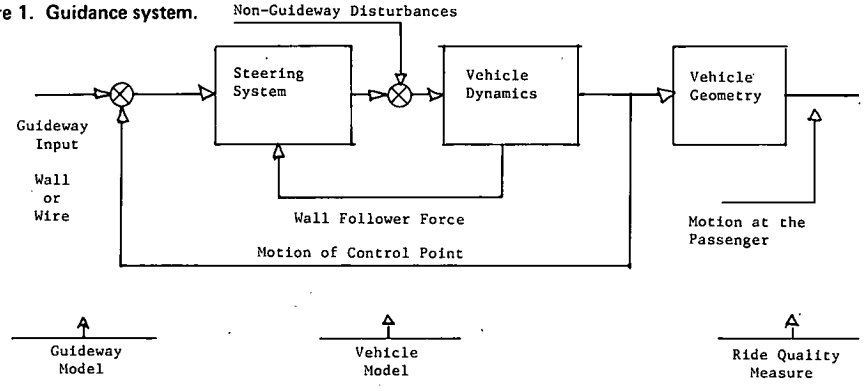

Figure 2. Standards for ride quality, reduced comfort boundaries, and lateral motion.

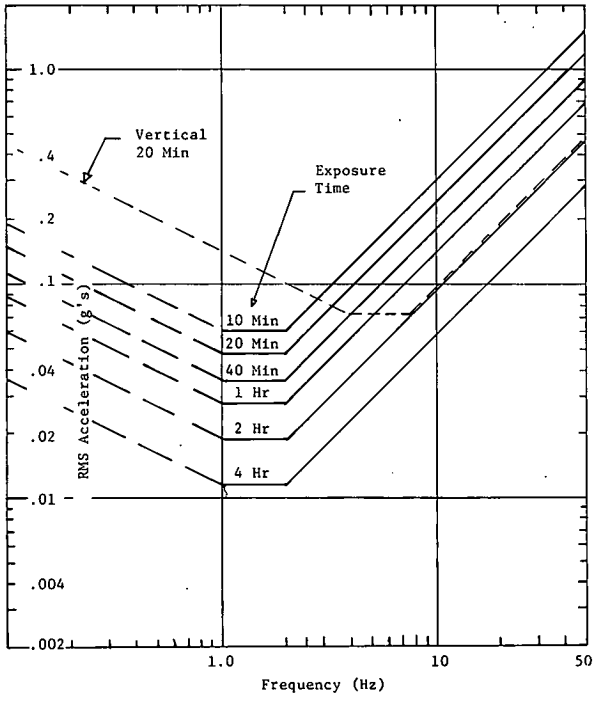

Figure 3. Low-frequency lag error.

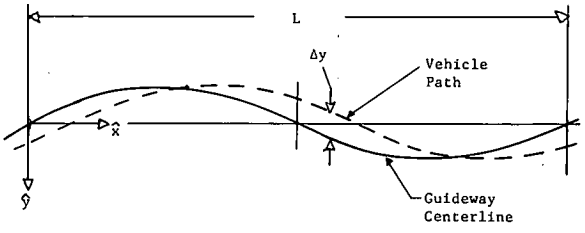

Figure 4. Servo steering system.

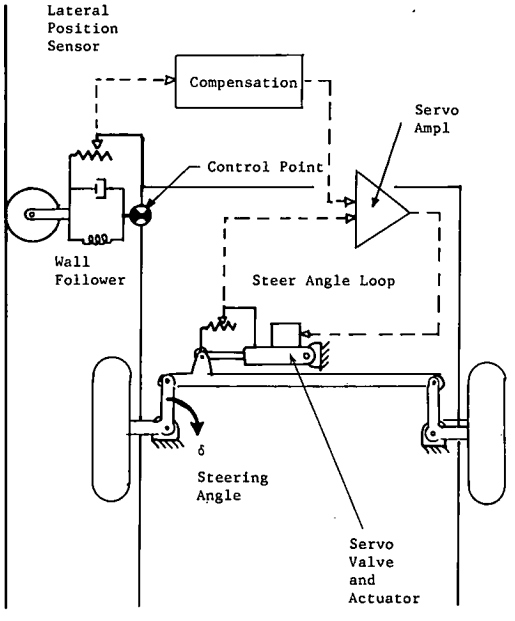

Figure 5. Herd steering system.

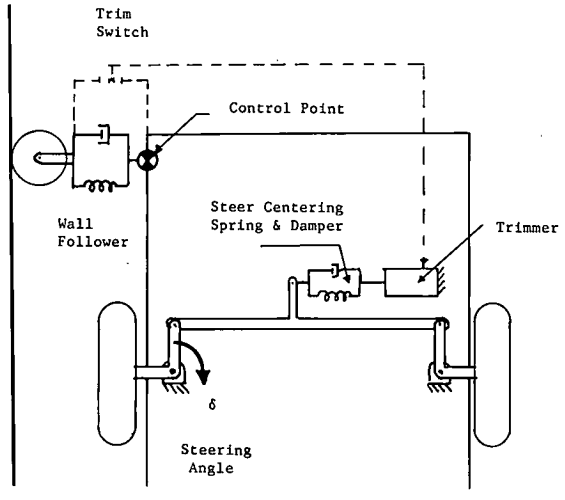

Figure 6. Variables of servo steering system.

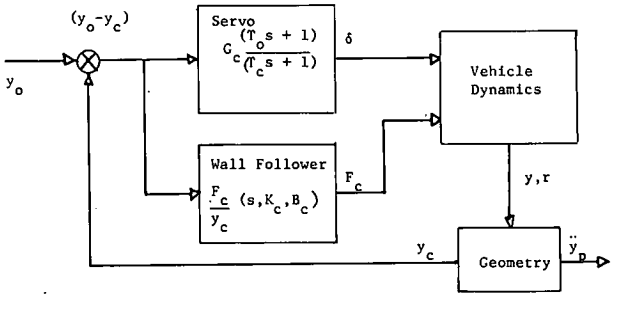

Table 1. Definition of symbols.

Symbol	Variable	Dimension
A	Guideway roughness factor	ft rad
a	Distance in y-direction from kingpin axis to center of tire patch in roadway plane	ft
B_o	Wall-follower damping coefficient	lb/(ft/sec)
B_s	Steering centering damping coefficient	ft·lb (rad/sec)
C	Study frequency range of 0.1 to 50 for evaluating acceleration spectra	Hz
C_1	Total tire lateral force coefficient, front wheel derivative of force with respect to slip angle	lb/rad
C_2	Total tire lateral force coefficient, rear wheel derivative of force with respect to slip angle	lb/rad
F_o	Total force on body from wall follower	lb
g	Acceleration of gravity	ft/sec^2
G_c	Lateral guidance loop gain	rad/ft
I	Total moment of inertia of vehicle and steering about center of gravity	slug·ft^2
I_s	Total moment of inertia of steering linkage about kingpin	slug·ft^2
j	Imaginary prefix, $\sqrt{-1}$	
K_o	Wall-follower spring constant	lb/ft
K_{sp}	Effective steering centering spring constant from kingpin inclination = a · Wt sin $\propto$ (small perturbation)	ft·lb/rad
K_s	Steering centering spring constant	ft·lb/rad
K_I	Trimmer gain	rad/sec·ft
ℓ_s	Distance in x-direction from kingpin axis to steering linkage mass center	ft
L	Wavelength of representative reverse curve	ft
m	Mass of total vehicle	slug
m_s	Mass of steering linkage	slug
M	Moment on steering linkage about kingpin	ft·lb
M_x	$\partial M/\partial x$, where x = v, δ, and r, and their time derivatives, partial derivative of steering moment about kingpin with respect to x (see Table 2)	
N	Moment about vehicle vertical axis	
N_x	$\partial N/\partial x$, where x = v, δ, and r, partial derivative of moment about vehicle z-axis with respect to x (see Table 2)	
r	Body angular rate about z-axis	rad/sec
s	Laplace operator	
T	Time period	sec
t	Time (variable)	sec
U	Forward velocity	ft/sec
v	Lateral velocity, $\dot{y}$, of vehicle	ft/sec
v_1	Local lateral velocity of front wheels	ft/sec
v_2	Local lateral velocity of rear wheels	ft/sec
W	ISO weighting factor for acceleration at passenger location	n
Wt	Total wheel load, front wheels	lb
x_1	Distance from body reference y-axis to kingpin center at road surface	ft
x_2	Distance from body reference to rear wheel center	ft
x_{cg}	Distance from body reference to total vehicle center of gravity	ft
x_{cc}	Distance from kingpin axis to center of tire patch in roadway plane = -R sin (θ)	ft
Y	Lateral force on vehicle	lb
Y_x	$\partial Y/\partial x$, where x = v, δ, and r, partial derivative of lateral force (y-direction) in vehicle coordinates with respect to x (see Table 2)	
$\ddot{y}_p$	rms lateral acceleration at passenger location	g
y_c	Lateral position of control point	ft
$\propto$	Kingpin angle	rad
δ	Steering angle	rad
δ_0	Steering reference angle (null)	rad
ζ	Damping factor	n
θ	Caster angle	rad
λ	Wavelength = $2\pi/\Omega$	ft
T_c	Servo steering time constant	sec
T_0	Lead compensation time constant	sec
ϕ	Vehicle yaw angle	rad
Φ_p	Spectral density of acceleration at passenger location	g^2/(rad/sec)
Φ_s	Spectral density of guideway input	ft^2/(rad/sec)
ω	Frequency	rad/sec
ω_n	Natural frequency	rad/sec
Ω	Spatial frequency	rad/ft

Table 2. Stability derivatives.

Symbol	Derivation	Symbol	Derivation
M_r	$Y_{r1}\, x_{cc} = \partial M/\partial r$	Y_δ	$-C_1$
M_v	$Y_{v1}\, x_{cc}$	$Y_{\dot\delta}$	$Y_{v1}\, x_{cc}$
M_δ	$Y_\delta\, x_{cc}$	Y_{v1}	C_1/U
$M_{\dot\delta}$	$M_v\, x_{cc}$	Y_v	C_2/U
N_r	$N_{r3} + N_{r2}$	Y_{r1}	$C\,(x_1 + x_{cc} - x_{cg})/U$
N_v	$N_{v1} + N_{v2}$	Y_{r2}	$C\,(x_2 - x_{cg})/U$
N_δ	$-C_1(x_1 + x_{cc} - x_{cg})$	N_{v1}	Y_{r1}
$N_{\dot\delta}$	$N_{v1}\, x_{cc}$	N_{v2}	Y_{r2}
Y_r	$Y_{r1} + Y_{r2}$	N_{r1}	$N_{v1}\,(x_1 - x_{cg})$
Y_v	$Y_{v1} + Y_{v2}$	N_{r2}	$N_{v2}\,(x_2 - x_{cg})$

Figure 7. Variables of herd steering system.

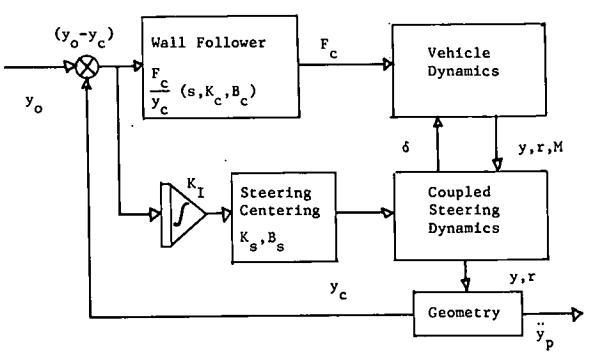

Figure 8. Coordinate and variable definition.

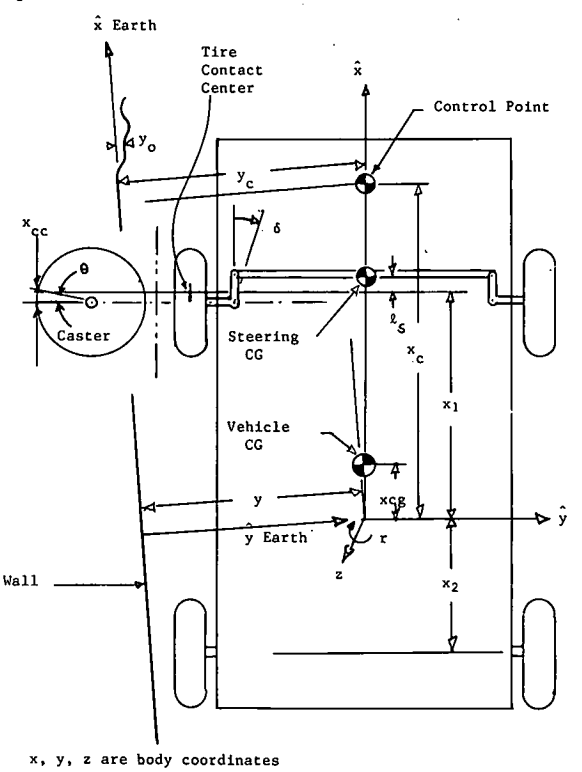

x, y, z are body coordinates

Figure 9. Basic vehicle dynamics: roots as function of speed.

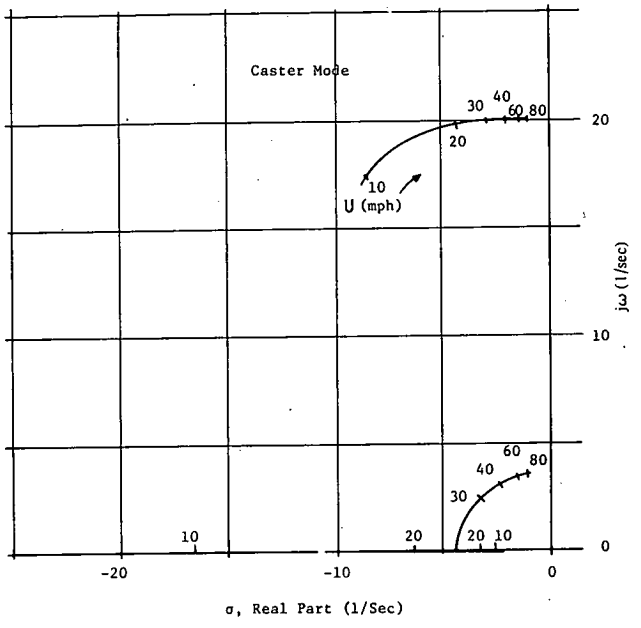

Figure 10. Servo steering: roots as function of gain and time constants (negligible wall-follower force).

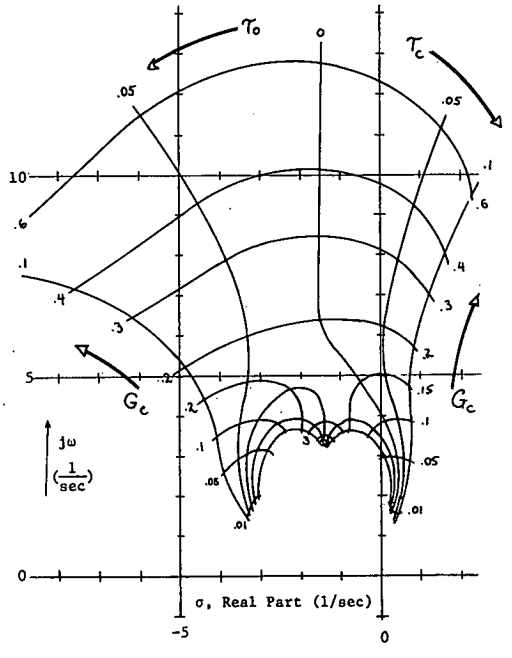

$$\Phi_p(j\omega) = \Phi_g(j\omega)\left[\frac{\ddot{y}_p}{y_0}(j\omega)\right]^2 \tag{23}$$

This gives the spectral density of acceleration at the passenger location, which is used to obtain the weighted rms value of acceleration discussed earlier.

$$\ddot{y}_p \text{ rms} = W(\omega)\left[\int_C \Phi_p(\omega)\, d\omega\right]^{1/2} \tag{24}$$

This is accomplished quite economically with adequate accuracy by simple numerical integration. The transfer function $\ddot{y}_p/y_0(\omega)$ is evaluated at $\omega = 0.25$ to obtain the phase shift for the low-frequency response measure.

The process is immensely more efficient than time-history simulation for parametric evaluation if for no other reason than the compactness of the output. The desired measures are computed directly and exactly,

Figure 11. Roots as function of gain and wall-follower stiffness.

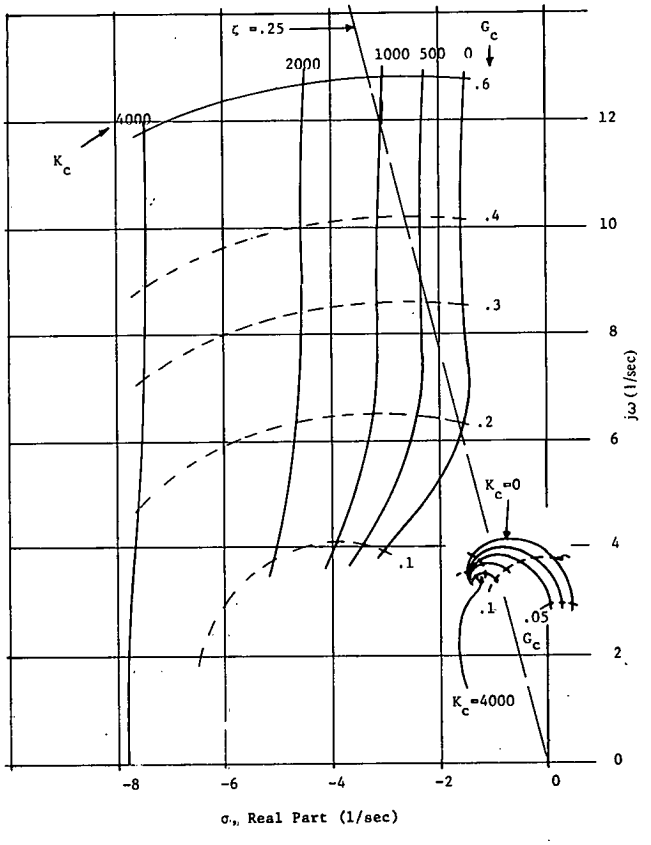

Table 3. Initial mapping parameters.

System	Symbol	Parameter Definition	Dimension	Mapping Range
Servo	G_c	Lateral guidance loop gain, $\delta/\Delta y$	rad/ft	0.05 to 6.0
	τ_o, τ_c	Servo and compensation time constants	1/sec	0 to 0.1
	K_c	Wall-follower spring stiffness, F_c/y_c	lb/ft	0 to 4000
	B_c/K_c	Wall-follower damping ratio (not ζ but $2\zeta/\omega$)	sec	0.1 to 0.4
Herd	K_c	Wall-follower spring stiffness, F_c/y_c	lb/ft	500 to 6000
	B_c/K_c	Wall-follower damping ratio (not ζ but $2\zeta/\omega$)	sec	0.1 to 0.4
	K_s	Steering centering spring constant, $M\delta/\delta$	ft·lb/rad	0 to 6000
	B_s	Steering centering damping coefficient	ft·lb/rad/sec	0 to 200
	K_i	Trimmer gain	rad/sec·ft	0 to 0.015

and a number of questions of accuracy and statistical significance are eliminated.

RESULTS AND CONCLUSIONS

Bare Vehicle Dynamics

The two-body model yields two oscillatory modes: a well-damped fundamental body mode and a poorly damped caster mode. Both exhibit constant natural frequency over the speed range and damping that decreases with speed (Figure 9). This representation assumes no mechanical friction within the steering system (only the normal force of the tire) and, therefore, reflects the minimum possible damping. Damping of this mode is easily controlled by a steering damper. Frequency is a function of the square root of the caster angle. The basic body mode reflects a near neutral steering relation, which is characteristic of the vehicle with full seated load. Preliminary exploration of the effect of center-of-gravity location showed that body dynamics is not strongly affected by loading changes.

Figure 12. Herd steering: roots as function of wall-follower stiffness and damping ratio (K_c and B_c/K_c) with no steering centering.

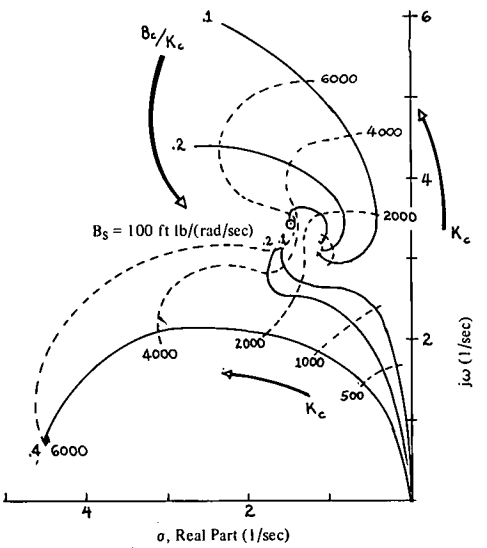

Figure 13. Herd steering: roots as function of wall-follower stiffness and damping ratio (K_c and B_c/K_c) with steering centering and trimmer.

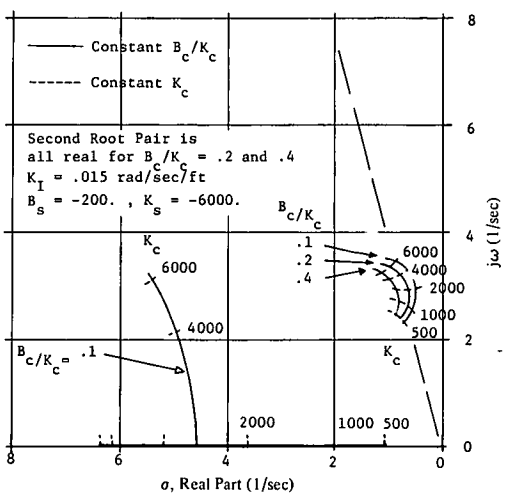

Parameter Study

The parameter study involves two levels of parameter variation: initial mapping at 60 mph and later one-dimensional exploration from a tentative optimum. The initial mapping parameters are given in order of importance in Table 3.

Stability

Basic Servo Loop

The root locus shown in Figure 10 provides some insight into the likely problems of the general system that feeds path error directly to steering angle of front-steered vehicles on free-running tires. In this plot, one parameter is gain, G_c. The other is a combination parameter: When it is zero, simple position feedback is represented. Values of τ_c represent system lag, a single lag inside the loop. In Figure 6, τ_c is kept at zero and τ_c is varied. Values of τ_c represent rate feedback with negligible controller lag. In this case in Figure 6, τ_c is kept at zero and τ_c is varied. These are two root pairs (oscillatory modes); one always tends to converge on the point (1.5, j3). In either case, we are concerned only with the one that crosses over into the right half plane. A zero value of τ_c should not be taken literally. It represents lead compensation to eliminate the effect of steering servo response lag. Two facts are evident: Low gain is unstable, and lag cannot be tolerated. No realistic steering servo lag will yield an adequately damped system unless velocity information is available. This has important implications for any mechanical linkage implementation of this principle. It is likely to be unstable. The essential problem is that any attempt to smooth the input, even the response of a pneumatic tire, will introduce enough lag in the loop to risk instability. Servo systems, on the other hand, will require lead compensation. Thus the system is highly sensitive to attempts

Figure 14. Herd steering: influence of wall-follower stiffness on passenger acceleration at different damping ratios.

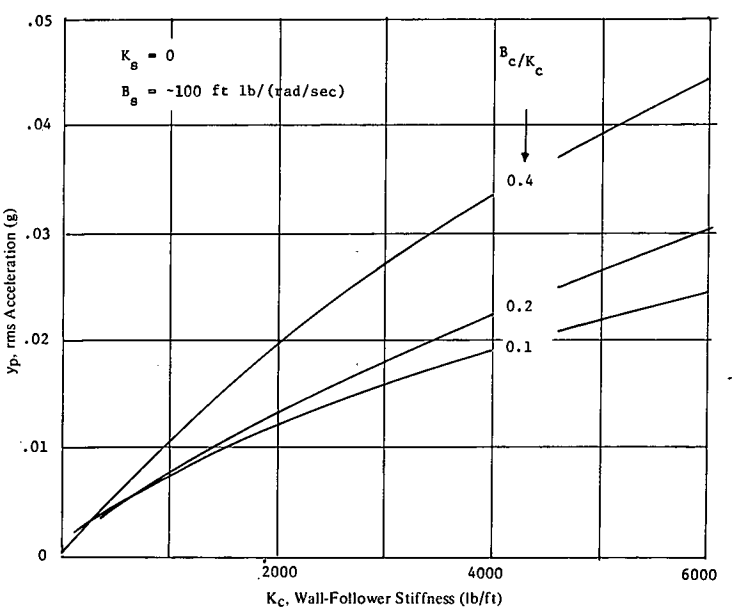

Figure 15. Servo steering: acceleration at passenger location as function of gain and compensation time constant.

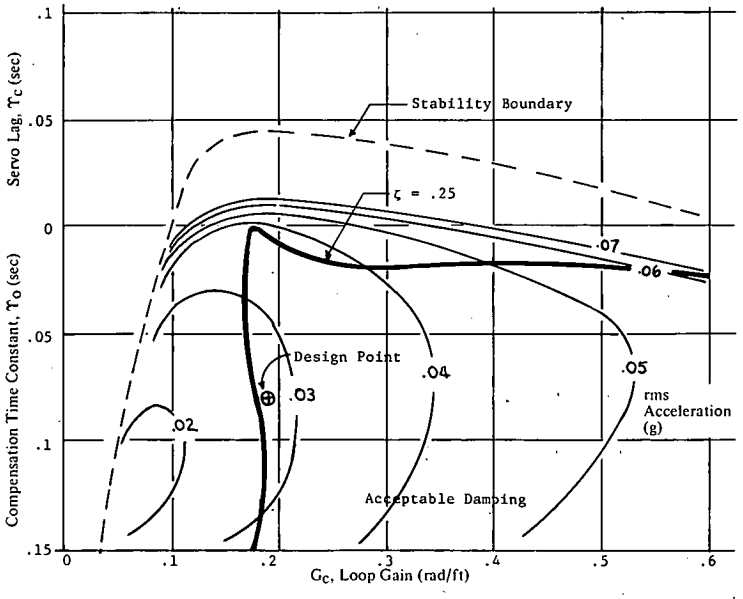

Figure 16. Herd steering: acceleration at passenger location as function of wall-follower stiffness and damping.

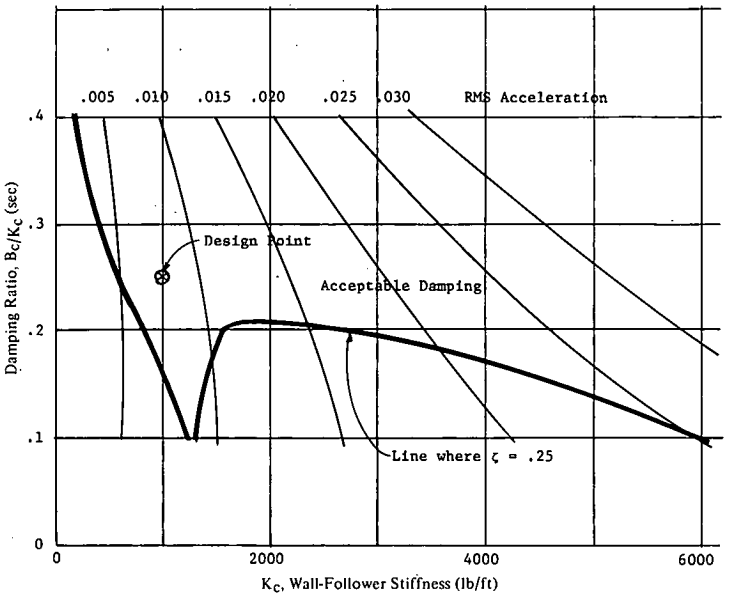

Figure 17. Servo steering: acceleration at passenger location as function of gain and wall-follower stiffness.

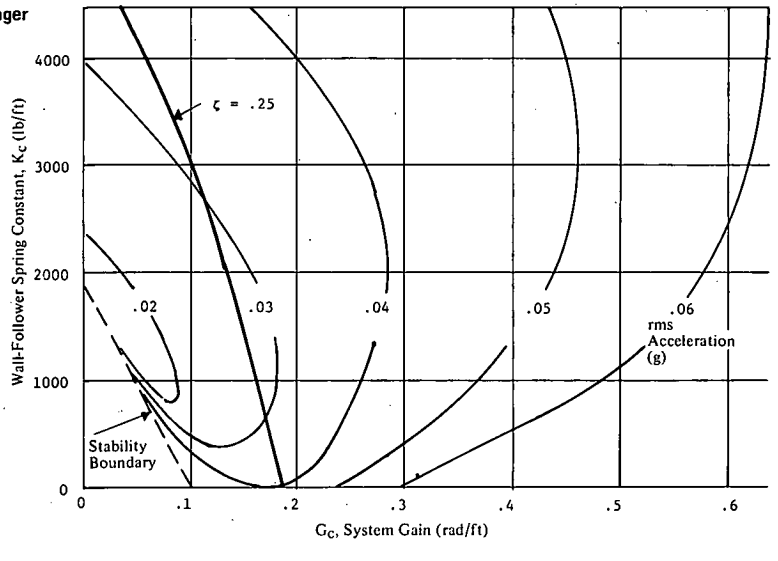

to isolate the vehicle from unwanted higher frequency components of wall irregularities. Unless cleverly implemented, they will turn out to introduce lag inside the loop.

Wall-Follower Force With Servo Control

Stiffness in the wall follower is effective in improving stability as long as adequate damping is provided. K_c is the parameter. Figure 11 shows the effect at $\tau_c = \tau_o = 0$. These time constants should not be interpreted literally. The configuration of combined servo and augmentation is realizable even with significant servo lag if lead compensation is selected to introduce negligible phase shift below frequencies of 6 to 8 rad/sec. The root locus maps gain, G_c, and wall-follower stiffness, K_c, at constant damping ratio, B_c/K_c. It shows a strong shift in the stable direction with increased stiffness.

Basic Herd Loop

The closed-loop roots for herd steering are mapped in Figure 12. To maintain a reasonable scale in the plots, the well-damped caster mode at about 23 rad/sec is not included. K_c acts like gain. The second parameter is B_c/K_c, wall-follower damping. This configuration has no steering spring centering, only a steering damper set at -100 ft·lb (rad/sec), Thus, it cannot be equipped with a trimmer. When the trimmer is included with a centering spring, the response map changes to that shown in Figure 13. The trend is to destabilize the basic body mode.

Summary of Stability Comparison

The servo system has strong tendencies toward instability at low gains; the herd system does not. Both systems

Figure 18. Comparison of acceleration at passenger location as function of steady-state path error.

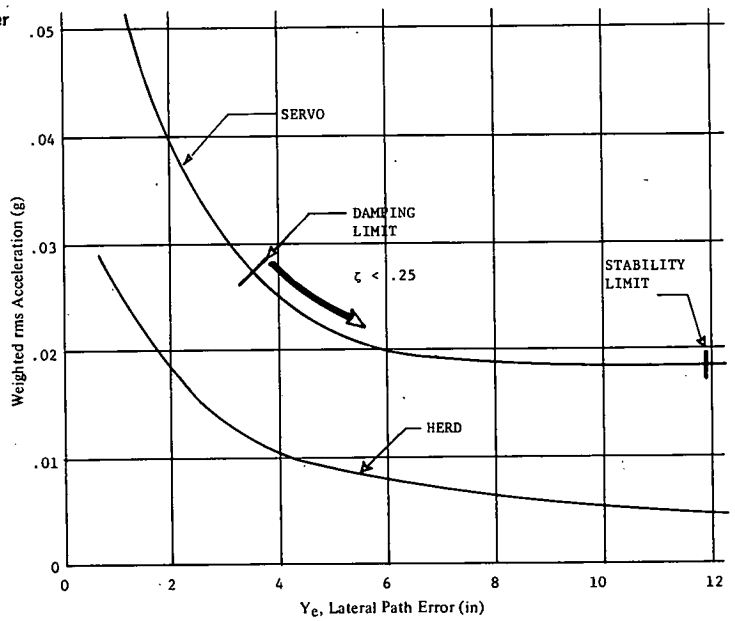

Figure 19. Comparison of acceleration at passenger location as function of low-frequency lag error.

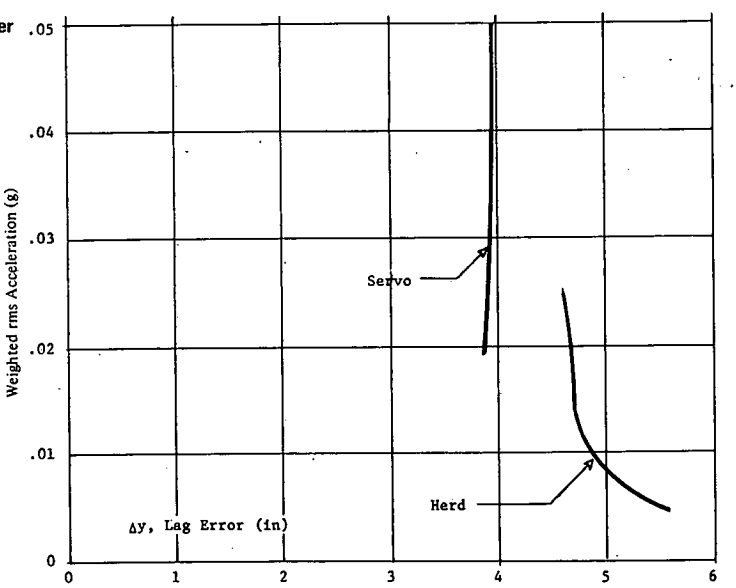

Figure 20. Comparison of acceleration spectra of servo and herd systems.

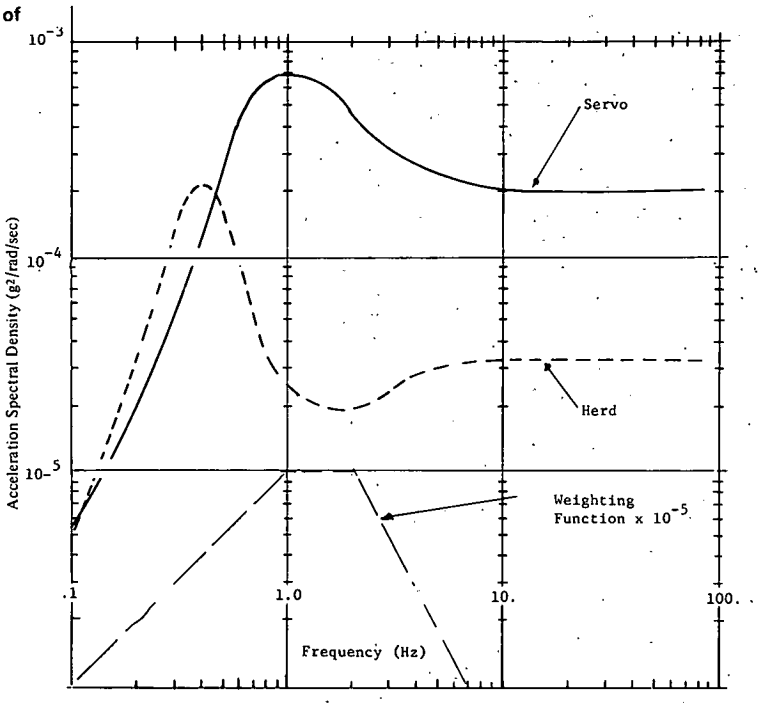

Figure 21. Servo steering: design point configuration roots as function of velocity.

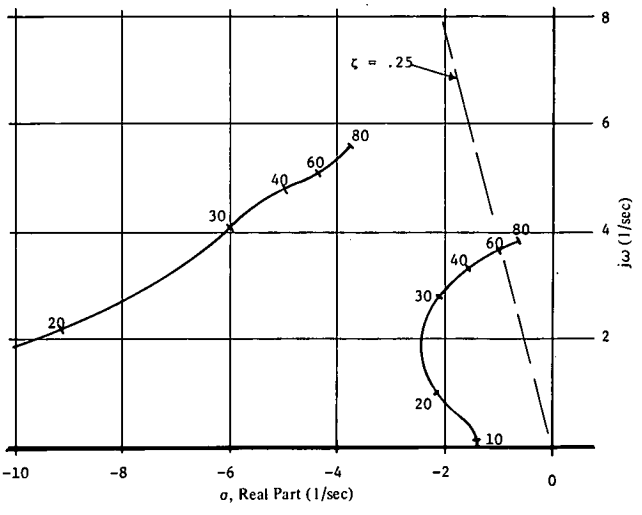

Figure 22. Herd steering: design point configuration roots as function of velocity.

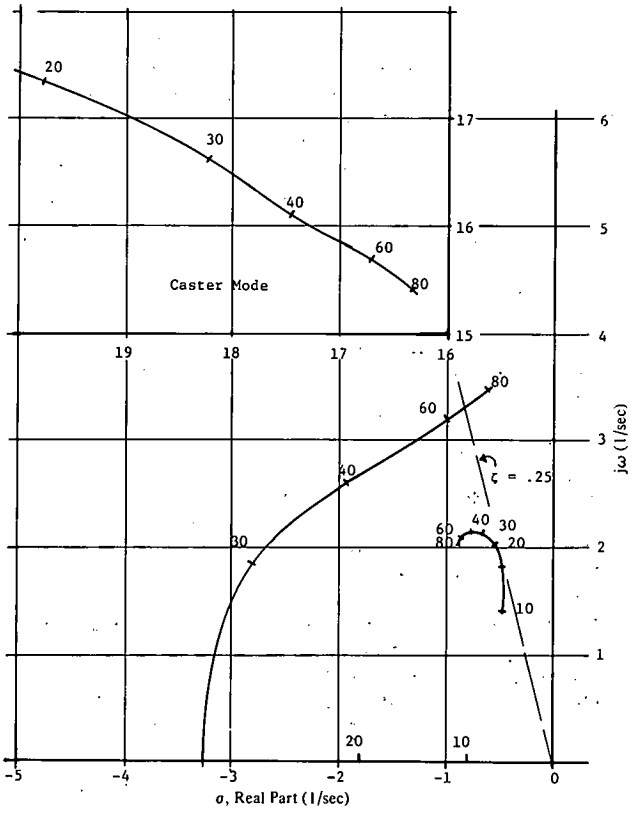

are capable of stable operation over a wide range of parameters. When the stability or damping standard of $\zeta = 0.25$ is applied, both systems are capable of complying. Both systems are improved by increased stiffness and damping of the wall follower.

Performance Comparison

In the parameter mapping process, the following performance measures were computed:

1. Roots of the system;
2. rms acceleration at the passenger location, $\ddot{y}_p$, the primary performance measure; and
3. Turn performance measures, steady-state error, y_e, and low-frequency lag error, Δy.

These measures can be plotted as functions of the

various parameters. For herd steering Figure 14 shows $\ddot{y}_p$ as a function of K_c at different values of B_c/K_c. These data can be cross plotted in a more informative way before the damping requirement is applied. Figures 15, 16, and 17 concentrate the information. Contours of constant passenger acceleration, $\ddot{y}_p$, are plotted as functions of the important parameters. This is read like a contour map. Stability and the damping standard are also mapped. This locates the line of minimum passenger acceleration in the two parameters. This line can then be plotted against the steady state or the lag error, whichever dominates. This final comparison is shown in Figures 18 and 19. The herd performance shown is accomplished without a trimmer; hence, the lateral error performance comparison is impartial.

The rms acceleration measurement, $\ddot{y}_p$, is a weighted integration over the spectrum. In accounting for the difference in performance, it is instructive to compare the spectra of the two at the selected design point. Figure 20 shows a comparison of the spectra and also the weighting pattern. The herd system exhibits a favorable dip of 1 to 2 Hz in response in the sensitive (heavily weighted) frequency range.

When a tentative design point has been established, a check can be made over the velocity range. The roots of the design point system as functions of velocity are shown in Figures 21 and 22. Single-dimension investigation of secondary parameters such as steering centering stiffness and damping can be performed to arrive at a more refined optimization.

The herd system shows a capability for superior ride quality; the acceleration levels are less than half those produced by an equivalent servo system. The servo system is penalized by the fact that stability demands are in direct conflict with the means for isolating the vehicle from unwanted guidance source irregularities. This effect may be counterbalanced in a full servo system by providing a guidance source other than the wall, which is easily made free of unwanted irregularities and maintained in that condition. This potential must be weighted against the potential for low cost, reliability, and maintainability of the passive steering approach.

REFERENCES

1. R. M. Hanes. Human Sensitivity to Whole-Body Vibration in Urban Transportation Systems: A Literature Review. Applied Physics Laboratory, Johns Hopkins Univ., TPR004, May 1970; National Technical Information Service, Springfield, Va., PB 192 257.
2. A. B. Broderson, H. E. von Gierke, and J. C. Guignard. Ride Evaluation in Aerospace and Surface Vehicles. Symposium on Vehicle Ride Quality held at Langley Research Center, July 1972, NASA, TM X 2620.
3. H. H. Richardson and others. Dynamics of Simple Air-Supported Vehicles Operating Over Irregular Guideways. Massachusetts Institute of Technology, Cambridge, June 1967; National Technical Information Service, Springfield, Va., PB 173 655.